

School of Computing
National University of Singapore



Graduate Research Paper

Reference Registration and Salient Surface Detection for Reconstruction of Deformed Skulls

by

Xie Shudong

under guidance of

A/Prof. Leow Wee Kheng

November, 2014

Contents

List of Figures	III
List of Tables	V
1 Introduction	1
1.1 Motivation	1
1.2 GRP Research Objectives	5
2 Related Work	7
2.1 Rigid Registration	7
2.1.1 Iterative Closest Point Registration	7
2.1.2 Fractional Iterative Closest Point Registration	8
2.1.3 Plane-Fitting Registration	9
2.2 Skull Reconstruction	10
2.2.1 Symmetry-Based Reconstruction	11
2.2.2 Geometric Reconstruction	13
2.2.3 Statistical Reconstruction	15

Contents	II
2.3 Summary	17
3 Plane-Fitting Registration	18
3.1 Plane-Fitting Registration Algorithm	18
3.2 Experiments and Discussions	21
3.3 Summary	25
4 Salient Surface Detection	27
4.1 Salient Surface Detection Algorithm	27
4.2 Experiments and Discussions	28
4.3 Summary	32
5 Continuing Research	33
5.1 Non-rigid registration	33
5.2 Salient Surfaces Detection	34
5.3 Weighting Parameter	34
5.4 Reconstruction of Deformed Skulls	34
6 Conclusion	36

List of Figures

1.1	Examples of skull deformities	2
1.2	Severely damaged skulls	3
1.3	Salient surfaces	4
1.4	The complex surface structure of a skull	4
2.1	An example of ICP registration	8
2.2	Example where FICP outperforms ICP	10
2.3	Registration on skull models	11
2.4	Symmetry-based reconstruction on the deformed skull	12
2.5	Framework for skull assembly and completion	13
2.6	Skull completion for the assembled skull	14
2.7	Geometric reconstruction for the incomplete medieval skull	14
2.8	Workflow of the outlier detection	16
3.1	Skull models	22
3.2	Convergence curves	25

3.3	Skull registration results	26
4.1	Salient surface detection	30
4.2	Salient surface extraction results	31

List of Tables

3.1	Comparison of registration methods	23
-----	--	----

Chapter 1

Introduction

1.1 Motivation

Skull deformities occur frequently in the world. Many patients suffer from skull fracture in traffic accidents. In Singapore, National University Hospital (NUH) alone receives about 250–350 patients with skull fracture every year. Also, some patients' skulls are congenitally deformed. Worldwide, one in 5,600 children is born with facial asymmetry [Hem10]. Moreover, some ancient skulls unearthed by archaeologists are incomplete and deformed due to natural forces or ancient religious purposes. Fig. 1.1 illustrates examples of skull deformities.

In addition to inaesthetic facial appearance, skull deformities may lead to incomplete functionalities because the muscles and skins attached to a deformed skull are also deformed [LP98]. For example, jaw deformity may lead to chewing problem by affecting the movement of the jaws [Che13]. Orbit (eye socket) deformity may affect the ability of the skull to support the eye ball and lead to impaired vision [Che13]. Skull deformities greatly affect the patients' quality of life and even threaten their lives. In forensics, the completeness of a skull is a valuable factor in successful identification of missing individuals. In archeology, skeletal remains excavated by archaeologists are often fractured into pieces due to environmental or animal activities. The analysis of the morphology of an-

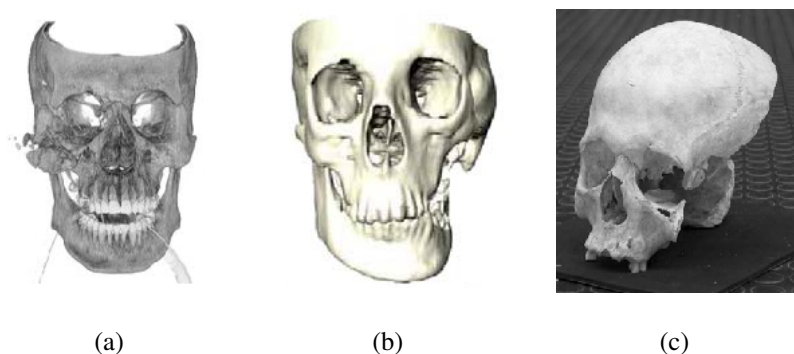


Figure 1.1: Examples of skull deformities. (a) Fractured skull due to accident [Che13]. (b) Congenitally deformed skull [ZLES05]. (c) Incomplete medieval skull [FdCP⁺08].

cient skulls is also conditioned by the integrity of the cranium. Therefore, reconstruction for deformed skulls is crucial and significant.

Skull reconstruction is a difficult task for surgeons, forensic investigators and archaeologists. Firstly, the normal shape corresponding to the missing or fractured part is unknown. When the unknown normal shape is complex, it takes time and effort to predict and generate the estimated shape for the fractured or missing part. Secondly, for a significantly damaged skull, there are usually plenty of missing or fractured parts to be repaired (Fig. 1.2). In this case, it is very time consuming for restorers to achieve the reconstruction. Due to these difficulties, computer-aided skull reconstruction is necessary and significant.

Skull reconstruction is also difficult for computation. Firstly, the shapes of human skulls vary greatly across different identity, age, gender and racial groups. Due to the skull variation, the unknown normal shape corresponding to the fractured or missing part can differ a lot among different skulls. Therefore, the estimation of unknown normal shape is challenging for computation, since a reconstruction algorithm should make the reconstruction as close as possible to the original undamaged skull no matter where the target skull is from. Secondly, to fill in the missing part with a normal shape, the reconstruction algorithm should ensure **surface continuity** which means that the salient surface of the normal part should be flushed with the salient surfaces of the input deformed skull. Salient surfaces of a skull include outer surfaces and surfaces around the eye sockets and other

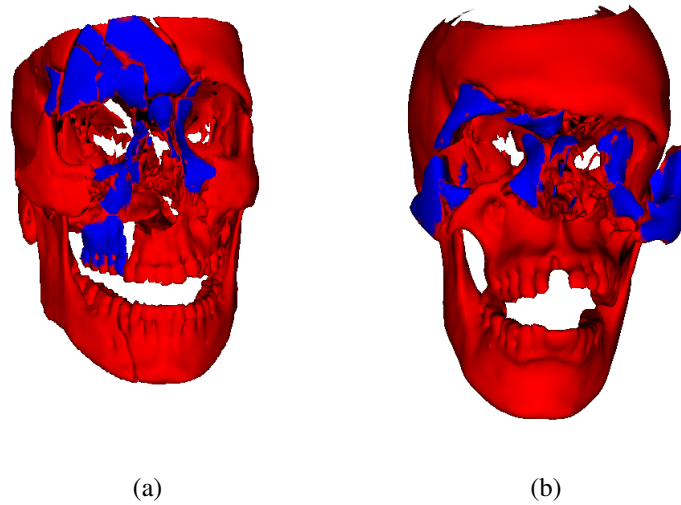


Figure 1.2: Severely damaged skulls with plenty of fractured parts (blue colored) to be repaired.

openings (Fig. 1.3). To guarantee **surface continuity**, the algorithm needs to deal with local details of skull surfaces. However, the local surface structure of a human skull is very complex. For example, as can be seen in Fig. 1.4, the surfaces contain many openings (e.g. openings around eye sockets). If the reconstructed bone is near the eye socket, it is difficult for the algorithm to check whether the bone is flushed with other undamaged surfaces or not. Therefore, it is difficult for the algorithm to ensure **surface continuity** of the reconstruction.

Existing approaches for skull reconstruction include symmetry-based reconstruction, geometric reconstruction and statistical reconstruction. Symmetry-based reconstruction [CSP⁺07, dMCP⁺06, LCL⁺03, CTS⁺10, FdCP⁺08, GWL99, BS11, LYW⁺11, YWML11] take advantage of the approximately left-right symmetry of human skulls. It uses the reflection of the part that is present on one side to fill in the missing part or replace the fractured part on the other side. Symmetry-based reconstruction methods are not applicable to skulls which are bilaterally deformed. Geometric reconstruction [BS11, LYW⁺11, YWML11, WYLL11, BSMG09, GMBW04, FdCP⁺08, Che13] register and deform a reference model to match the shape of the target model and replace the fractured part or fill in the missing region by its corresponding part on the reference model. Geometric re-

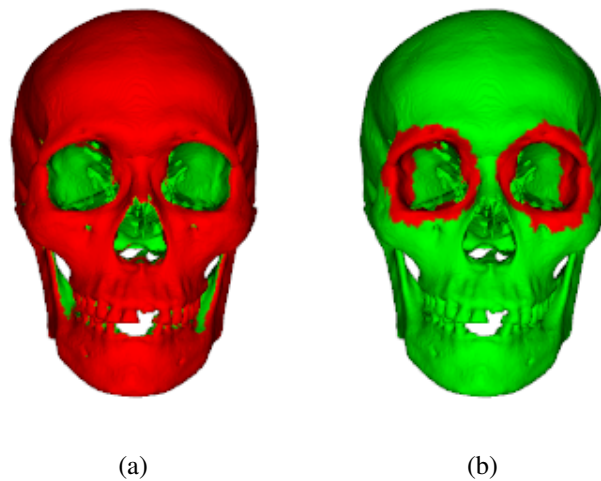


Figure 1.3: Salient surfaces (red color). (a) Outer salient surfaces that can be identified automatically. (b) Salient surfaces around eyes sockets that are difficult to detect.

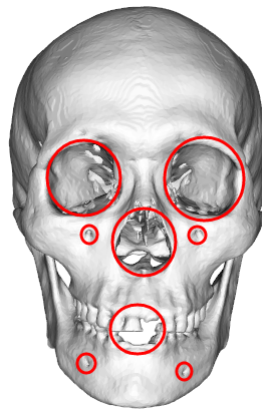


Figure 1.4: The complex surface structure of a skull. The surface contains many openings, which makes it hard for computation to ensure **surface continuity** if the reconstructed bone is around the openings.

construction uses single reference model, which is insufficient for reconstructing skulls because the detailed shapes of human skulls differ significantly with different identifies, genders, ages and races. Statistical reconstruction [LAV09, ZLES05, Zha14] generate the estimated model for the deformed skull by changing shape parameters of the statistical model and fill in the missing part or replace the fractured part with its corresponding part on the estimated model. Each shape parameter of the statistical model adds overall changes to the mean skull shape. Therefore, statistical reconstruction focuses on global structures

rather than details of local features, which may lead to mismatches between normal parts of the input skull and the reconstructed skull [Zha14].

A good reconstruction approach should be robust, accurate and able to deal with the limitations discussed above. Firstly, it should be robust enough to handle incomplete and deformed skulls. It should produce correct reconstruction for the fractured bones or missing parts in the target model. Secondly, a good reconstruction approach should yield accurate result. In practice, it is impossible to measure accuracy without ground truth, so we expect the reconstruction to at least satisfy some properties that we know about normal skulls. These properties include, for example, **skull normality** which means the reconstructed model should look like a normal human skull, and **surface continuity** which means the salient surfaces (Fig. 1.3) of a reconstructed skull should be flushed with the salient surfaces of the input deformed skull. Satisfying these properties should contribute to accurate reconstruction.

1.2 GRP Research Objectives

The overall research goal is to develop a robust and accurate method for reconstructing normal skulls from severely deformed ones. First of all, a reference model is needed. A reference model provides information about the shape of a normal skull, salient surfaces, anatomical landmarks and lateral symmetric plane. Moreover, a reference model represented by a statistical model can also provide information about variation of normal human skulls. These information are potentially useful for the deformed skull reconstruction. To utilize the information, the reference model needs to be aligned to match the shape of the target model so that the information on the reference model can be applied onto the target model. A perfect alignment that matches the shape of the reference model and the target model requires non-rigid registration. In addition to matching shapes, non-rigid registration also needs to take care of the size, position and orientation of the models. So, this paper focuses first on rigid registration, and non-rigid registration will be studied in subsequent research.

[Che13] presents a rigid registration method specialized for human skulls. The work compares its method with 2 other rigid registration methods on 3 fractured skulls, which is not enough to show its robustness and accuracy. So, this paper performs a benchmark test on more skull models to evaluate the accuracy of the three methods.

Secondly, in reconstructing a normal skull from a deformed skull, the salient surfaces of the reconstructed skull should flush with salient surfaces of the normal parts of the deformed skull. Salient surfaces include outer surfaces and surfaces around eye sockets and other openings (Fig. 1.3). Outer surfaces are easy to detect automatically, while the automatic detection of salient surfaces around eye sockets and other openings are more difficult to achieve. A fully automatic algorithm for salient surface detection would contribute to the research on reconstructing deformed skulls.

Based on the discussion above, two objectives are identified for the initial GRP research:

- Perform benchmark test on the three rigid registration methods reported in [Che13]. Quantitative analysis is needed to evaluate the accuracy of the three methods.
- Develop a method that automatically extracts salient surfaces on a skull. The method must work for both normal skulls and incomplete, deformed skulls. The developed method should identify both the outer surfaces and the surfaces around eye sockets and other openings automatically.

Chapter 2

Related Work

Many existing work about skull reconstruction involves rigid registration. A robust rigid registration is significant to skull reconstruction, as the accuracy of rigid registration can affect the performance of the reconstruction result. This chapter will talk about rigid registration (Sec. 2.1) and skull reconstruction (Sec. 2.2).

2.1 Rigid Registration

Existing rigid registration methods include Iterative Closest point (ICP), Fractional Iterative Closest Point (FICP) and plane-fitting registration. All these algorithms can work without knowing the correspondence between two models.

2.1.1 Iterative Closest Point Registration

Iterative Closest Point (ICP) [BM92] is an effective algorithm for rigid registration without knowing the correspondence. It is an iterative algorithm that repeatedly guesses the correspondence between the reference model and the target model and computes the best similarity transformation between them. ICP is summarized in Algorithm 2.1.

Algorithm 2.1: Iterative Closest Point (ICP) registration algorithm

Repeat until convergence:

1. For each point on the reference model, find its closest point on the target model.
2. Compute the similarity transformation using the correspondence points.
3. Apply the similarity transformation to all points of the reference model.

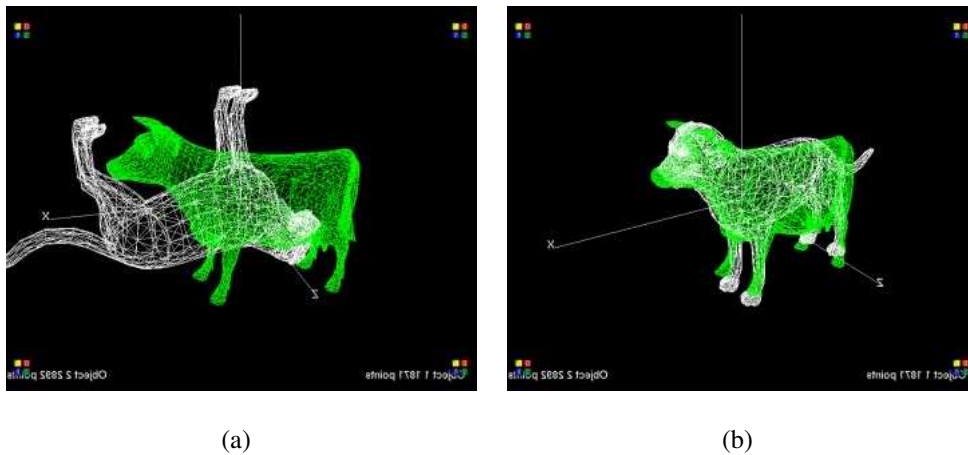


Figure 2.1: An example of ICP registration. (a) Before registration. (b) After registration.

ICP does not rely on any parameters, which enables it to work automatically. It can achieve good performance for normal models (Fig. 2.1). However, one weakness of ICP is that it is not robust to noise. It could fail when there are many outliers or missing parts in the target model.

2.1.2 Fractional Iterative Closest Point Registration

Fractional Iterative Closest Point (FICP) algorithm [PLT07] is a variant of ICP that is robust to outliers and missing data. Similar to ICP, FICP also computes the best similarity transformation iteratively that registers the reference model to the target model. ICP registration does not work when the target model contains a large number of outliers, since

Algorithm 2.2: Fractional Iterative Closest Point (FICP) registration algorithm

Repeat until convergence:

1. Find correspondence between the reference model and the target model.
2. Find the inlier subset of the reference model.
3. Compute similarity transformation using correspondence of points in the inlier subset.
4. Apply the transformation on all points of the reference model.

it blindly finds correspondence for all points of the reference model, which may involve a large number of outliers on the target model. To make the registration robust, FICP registration algorithm computes the transformation using only the inlier set which is a subset of reference model points that have the smallest distances to the target model. The algorithm is summarized in Algorithm 2.2.

FICP algorithm is more robust than ICP. Fig. 2.2 shows an example where FICP registration outperforms ICP registration.

2.1.3 Plane-Fitting Registration

Plane-fitting registration [Che13] is a rigid registration algorithm specialized for laterally symmetric models such as human skulls. It is more robust than existing rigid registration algorithms such as ICP and FICP. Although FICP algorithm is robust to outliers, it is not suitable for registering deformed skulls because it does not take into account anatomical structure of the skulls. As a result, the parts of the reference model does not match to the anatomically correct parts of the deformed skull. Plane-fitting registration achieves its robustness by ensuring that the symmetric plane of the reference model is registered to the

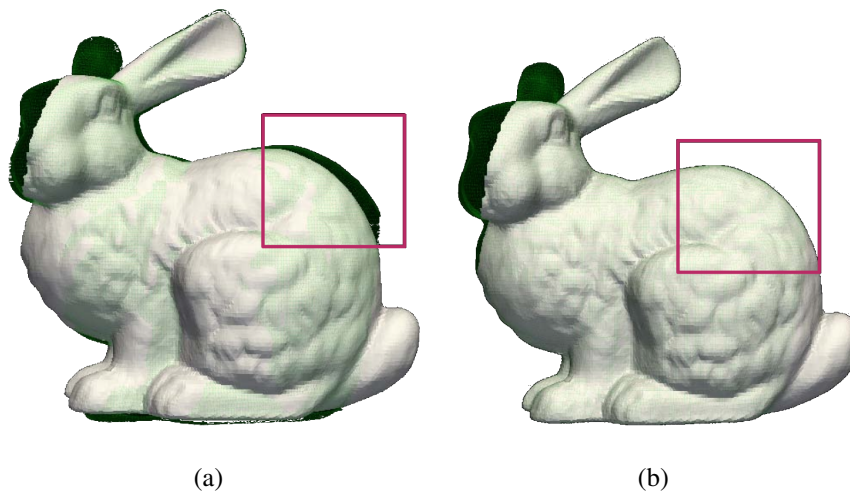


Figure 2.2: Example where FICP outperforms ICP. (a) ICP registration. Two models did not fit well since ICP registration is influenced by the missing data. (b) FICP registration. The reference matched the target model well.

planar landmarks (i.e. landmarks on the mid plane of the target model).

Plane-fitting registration is an extension of FICP algorithm. In each iteration, it finds correspondence between the reference model and the target model using not only mesh vertices but also the planar landmarks. The correspondence for the plane landmarks serves as a constraint that enhances the matching of the mid plane between two models. As a consequence, plane-fitting registration may yield better registration result than FICP on skull models (Fig. 2.3). In [Che13], plane-fitting registration algorithm is tested on 3 fractured models, which is not enough to prove its robustness. As a reason, benchmark test will be done on ICP, FICP and plane-fitting registration to see which method is more suitable for skull registration.

2.2 Skull Reconstruction

Existing approaches for skull reconstruction include symmetry-based reconstruction, geometric reconstruction and statistical reconstruction.

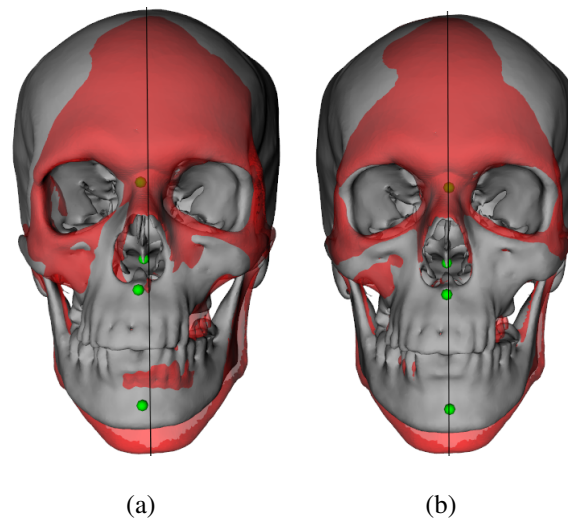


Figure 2.3: Registration on skull models and plane-fitting registration is better. (a) FICP registration. There is a mismatch on the mandible. (b) Plane-fitting registration. The skull models fit well.

2.2.1 Symmetry-Based Reconstruction

Human skulls can be considered as approximately left-right symmetric with respect to the Mid-Sagittal Plane (MSP) which is the vertical plane through the midline of the skull. Symmetry-based reconstruction methods [CSP⁺07, dMCP⁺06, LCL⁺03, CTS⁺10, FdCP⁺08, GWL99, LYW⁺11, YWML11] use the reflection of the normal part on one side of the skull to replace the fractured part or fill in the missing part on the other side.

For example, the work in [LCL⁺03] uses symmetry-based reconstruction approach for implant design. The mirrored image of the healthy part is used as the implant for the deformed part. The authors apply this method to generate implant for an eight years old boy with a large defect on the left side of skull. The implant surgery is successful and the postoperative recovery is smooth.

In the work of [FdCP⁺08], some parts on the left side of the medieval skull are missing (Fig. 2.4). The reflection of the healthy part on the right side of skull is used to cover the missing part on the left side. Then their algorithm deforms the mirrored part to fit the skull better, completing the reconstruction.

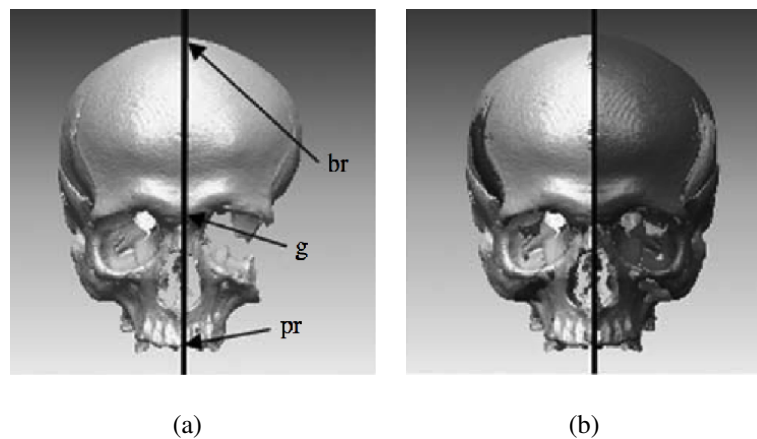


Figure 2.4: Symmetry-based reconstruction on the deformed skull [FdCP⁺08]. (a) Original skull model with some parts on the left side of the face missing. (b) Normal model constructed by reflecting the right side to the left side.

The work of [CSP⁺07, CTS⁺10] uses symmetry-based reconstruction in their computer-aided surgery system. Users can cut abnormal parts of a skull and reflect normal parts with respect to the mid-sagittal plane (MSP) to cover the missing regions.

The method in [LYW⁺11] uses symmetry-based reconstruction approach to iteratively refine the estimated shapes corresponding to the missing parts of an incomplete skull until the symmetry error of the reconstructed model is minimal. To begin with, the missing parts of the target skull model are filled in by their corresponding parts on a reference model. Then during each iteration, the reflection of the repaired target skull model with respect to the symmetry plane, which is identified automatically, is set as the new reference model. The missing parts of the repaired target model are filled in by their corresponding parts on the new reference model.

The work in [YWML11] uses symmetry-based reconstruction approach to fill in missing parts when it is possible. For those which cannot be filled in by symmetry-based reconstruction, they are filled by their corresponding parts from a reference model.

Symmetry-based reconstruction is a simple and useful approach that is widely used in computer-aided surgery planning systems and has been successfully applied to many real

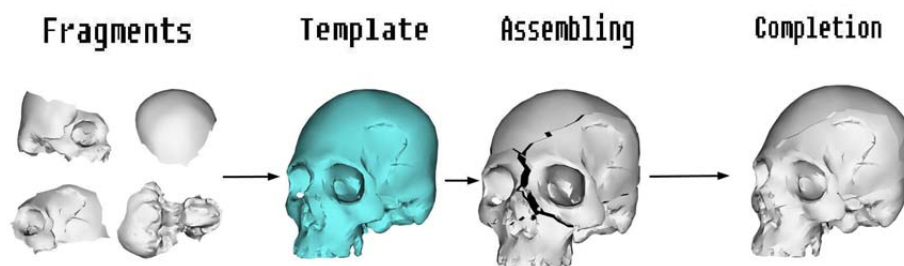


Figure 2.5: Framework for skull assembly and completion [WYLL11].

cases. However, it cannot be applied directly to a deformed skull with bilateral defects.

2.2.2 Geometric Reconstruction

Geometric reconstruction [BS11, LYW⁺11, YWML11, WYLL11, BSMG09, GMBW04, FdCP⁺08, Che13] registers and deforms a reference model to match the shape of the target model and replaces the fractured part or fills in the missing part with their corresponding parts on the reference model.

[WYLL11] proposes a framework for skull assembly and completion (Fig. 2.5). The framework computes rigid registration from fragments to a reference model in order to determine the spatial relationship between the fragments for assembly. Since the assembled skull is usually incomplete, skull completion operation is needed to refine the reconstruction (Fig. 2.6). To begin with, it computes non-rigid registration from a reference model to the assembled skull, which deforms and aligns the reference model to the assembled skull. The missing part on the assembled skull is filled in by its corresponding part on the reference model. Finally, surfaces between the filled-in patch and the assembled skull are flushed to make the surface continuous.

[BSMG09] is another example of geometric reconstruction from the field of forensic identification. The goal of their work is to deform a reference model to estimate the shape of an incomplete medieval cranium. It is almost impossible to reconstruct the original shape of the cranium due to its poor condition (Fig. 2.7). To reconstruct the skull, an

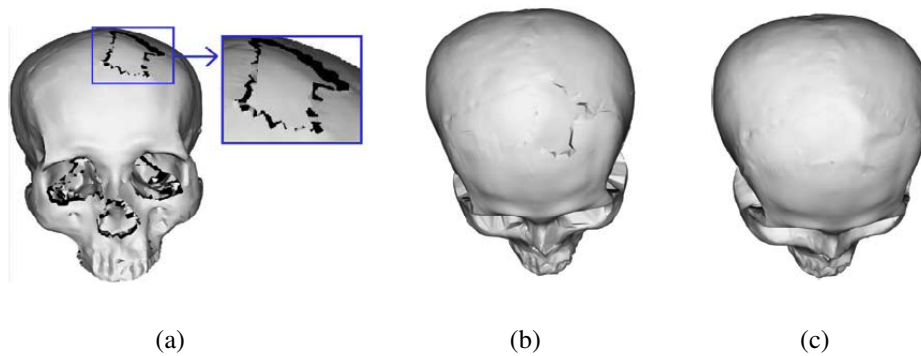


Figure 2.6: Skull completion for the assembled skull [WYLL11]. (a) The incomplete skull and the deformed template patch. (b) Gluing the patch by connecting boundary vertices and generating triangle faces between the patch and the assembled incomplete skull. (c) Smoothing the patch.

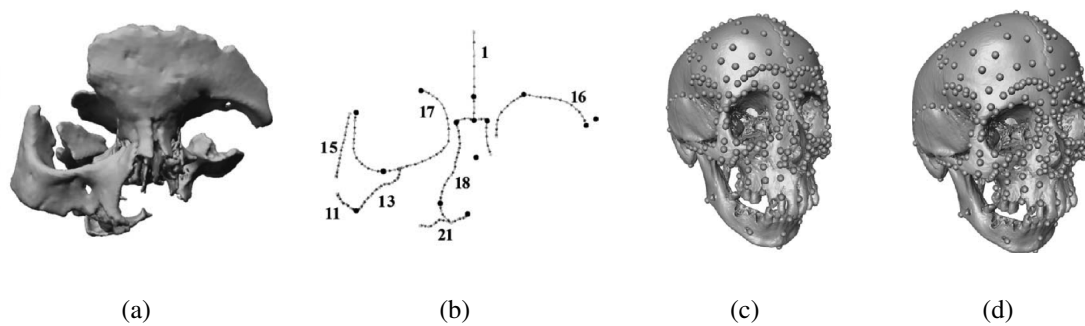


Figure 2.7: Geometric reconstruction for the incomplete medieval skull [BSMG09]. (a) incomplete cranium. (b) landmarks of the incomplete cranium. (c) reference model and its landmarks. (d) skull reconstruction by warping landmarks of the reference model towards those of the cranium.

intact skull with similar appearance and same gender is selected as the reference model. Their algorithm deforms the reference model using Thin-Plate Spline (TPS) by moving its landmarks towards those of the cranium. The deformed reference model serves as an approximation for the target skull.

The work in [BS11] compares three reconstruction methods for incomplete skulls with each left cheek bone of them missing. The first method and the second method are both symmetry-based reconstruction. The third method warps a reference model onto the tar-

get skull model using Thin Plate Spline (TPS) and uses the warped model to repair the missing cheek bone. Experiment shows that the third method yields better results than the symmetry-based methods.

[Che13] uses Laplacian deformation to deform the salient surfaces (Fig. 1.3) of the reference model to estimate the normal surfaces of patient's skull model. Experiments are conducted in the work to examine the characteristics of normal skulls. It discovers that a feature measuring local variation is small between two normal skulls. Based on this observation, it registers and deforms the salient surfaces of the reference model by minimizing the local variation of difference. The estimated normal surface is continuous since the salient surface of reference model is continuous.

The basic idea of geometric reconstruction is to use a reference model to repair the target model. Usually the first step is to align the reference model to the target model using rigid registration. Then the reference model is deformed to fit the shape of the target model in order to repair it. Geometric reconstruction is applicable to skulls with bilateral deformities, and it overcomes the limitation of symmetry-based reconstruction. The selection of reference model is essential as it determines the accuracy of reconstruction. However, geometric reconstruction uses single reference model, which is insufficient for reconstructing skulls because detailed shapes of human skulls differ significantly with different identifies, genders, ages and races.

2.2.3 Statistical Reconstruction

Statistical reconstruction generates the estimated model for the deformed skull by changing shape parameters of the statistical model. Then it replaces the fractured part or fills in the missing part of the target skull model with its corresponding part on the estimated model.

[LAV09] reconstructs estimated shapes for missing parts of incomplete skulls using a statistical model based on a robust variation of PCA. The statistical model is suitable for deformed skull reconstruction since it can be built from low quality data sets with artifacts and missing information. To begin with, given a training set of skulls, a complete and

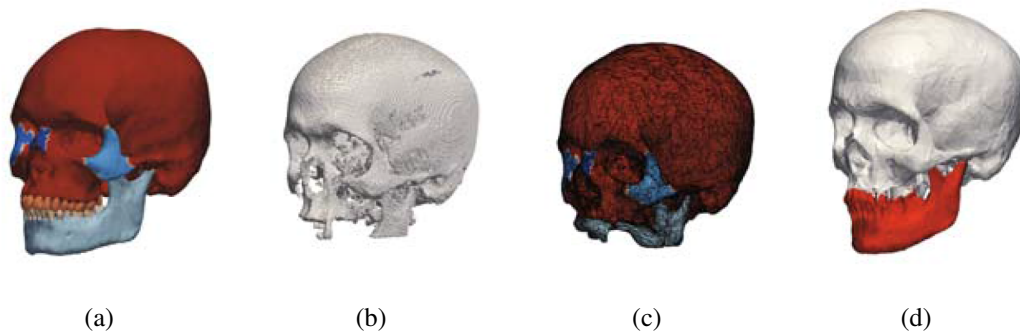


Figure 2.8: Workflow of the outlier detection [LAV09]. (a) A reference model is segmented into parts based on anatomy (b) Some shapes used for model building are incomplete or noisy. (c) The reference is warped to match the shape of the target. The missing parts lead to an unnatural deformation and can thus be identified as outliers. (d) The outlier parts are reconstructed from the remaining data.

normal model is singled out as the reference model, which is then segmented into parts based on anatomical structure (Fig.2.8). The authors assume that every target model can be obtained by deforming the reference surface with a smooth vector field which can be computed by a non-rigid registration algorithm based on Thirion’s Demons algorithm [Thi98]. The reference model is deformed by the computed vector field for each model in the training set in order to detect the outliers and missing data. Outliers are marked as missing, and the remaining parts of each model are used for building the statistics shape model using Probabilistic PCA (PPCA) [Row98, TB99]. According to the authors, PPCA is fast and able to estimate the missing data with maximum likelihood. For each target model, the missing parts can then be reconstructed by searching for the best shape parameters for the statistical shape model.

Active Shape Model (ASM) [CTCG95] is by far the most popular statistical shape model, which has been adopted in [Zha14] for skull reconstruction. To build ASM, the training models need to be resampled by computing the correspondence between them using the algorithm proposed in [ZCL13] such that all of them have the same number of vertices and connectivity. The resampled training models are then aligned together spatially using Procrustes analysis [Goo91, Gow75]. The aligned models are used to build

the active shape model. Given a target deformed skull model, the algorithm searches for optimal shape parameters to minimize the shape error between the generated model and the target model. The model generated from optimal shape parameters serves as the reconstruction of the target skull.

Statistical reconstruction generates estimated shape by changing shape parameters of statistical models, which overcomes the limitation of geometric reconstruction as it can handle the significant variation of human skulls. However, statistical reconstruction focuses on global structures rather than details of local features because the shape parameters govern overall changes to the mean skull shape. This may cause the surfaces of the reconstructed model and the normal parts of the deformed model to be mismatched.

2.3 Summary

The methods for model reconstruction include symmetry-based reconstruction, geometric reconstruction and statistical reconstruction. Symmetry-based reconstruction is not applicable when the target skull model has bilateral defects. Geometric reconstruction uses single reference model, which is insufficient for reconstructing skulls because detailed shapes of human skulls differ significantly across different genders, ages, identities and races. Statistical reconstruction focuses on global structures rather than details of local features, which may cause the surfaces of the reconstructed model and the normal parts of the deformed model to be mismatched.

Registration plays an important role in the field of skull reconstruction. Although Iterative Closest Point (ICP) works well in many cases, it yields poor results when there are significant outliers. Fractional Iterative Closest Point (FICP) is robust to outliers, but it does not take into account the anatomical constraint. As a result, FICP is not that suitable for deformed skull registration. Plane-fitting registration incorporates the advantages of FICP and the mid-sagittal plane constraint, which may produce better results than FICP on skull models.

Chapter 3

Plane-Fitting Registration

Plane-fitting registration [Che13] registers a reference model to the target model such that the landmarks on the target model are as close as possible to the symmetric plane of the reference model. It is more robust than existing registration algorithms such as ICP [BM92] and FICP [PLT07]. It achieves its robustness by ensuring that the symmetric plane of the reference model is registered to the planar landmarks on the target model. This makes it a promising rigid registration algorithm for deformed skull models.

3.1 Plane-Fitting Registration Algorithm

Plane-fitting registration is a robust algorithm that registers a reference model to match the target model. Reference model and target model can differ in size and shape details, due to deformation caused by injury, normal variation between individuals and possible incomplete scanning of the target skull. The registration algorithm should be robust to these variations, and find the common parts between the two models to align them.

Plane-fitting registration algorithm is an extension of the Fractional Iterative Closest point (FICP) [PLT07]. FICP does not ensure the matching of anatomic parts between the reference model and the target model. To overcome this limitation, plane-fitting registration algorithm enforces the matching of the reference plane to the planar landmarks on the

target model by forcing the planar landmarks on the target model as close as possible to the MSP of the reference model. Given a reference model F and a target model D with unknown correspondence, FICP minimizes a fractional mean-square distance [PLT07]:

$$E_1 = \left(\frac{|F|}{|G|} \right)^\lambda \frac{1}{|G|} \sum_{p \in G} \|T(p) - c(p)\|^2 \quad (3.1)$$

where G is a subset of F containing only the inliers, $c()$ is the correspondence mapping function of p that finds p 's closest point on the target model, λ is a constant parameter with positive value, and $T()$ is the similarity transformation to be optimized. By minimizing E_1 , FICP finds a large inlier set G with small errors and outputs the transformation computed only on G .

In addition to the fractional mean-square distance (Eq.3.1), plane-fitting registration introduces a plane-fitting error E_2 to the objective function:

$$E_2 = \frac{1}{|L|} \sum_{v \in L} d_\pi^2(v) \quad (3.2)$$

where L is the set of planar landmarks on the target model, and $d_\pi(v)$ is the distance from v to the symmetric plane of the transformed reference model F . The overall objective function to be minimized becomes:

$$E_r = E_1 + E_2 \quad (3.3)$$

There is no weighting parameter between E_1 and E_2 . In E_1 , except for the factor $(|F|/|G|)^\lambda$, it measures the mean distance between corresponding points, which is similar to E_2 that measures the mean distance between landmarks and the lateral symmetric plane. The term factor $(|F|/|G|)^\lambda$ ranges from 2 to 27 in our experiment, which means E_1 and E_2 could be unbalanced. So, adding a weighting parameter α to E_1 might be necessary. Then the equation becomes

$$E_r = \alpha E_1 + E_2$$

A straightforward way to balance E_1 and E_2 is to set α to $\left(\frac{|F|}{|G|}\right)^{-\lambda}$. But this will cancel the factor $(|F|/|G|)^\lambda$ in E_1 , which may affect plane-fitting registration's robustness to noise. Therefore, determining the balancing parameter α is a challenging task. So, this paper omits the α on now, and leaves it to continuing research work.

Algorithm 3.1: Plane-fitting registration algorithm

Repeat until convergence:

1. Find correspondence between F and D using mesh vertices and plane landmarks. Denote $q \in D$ as corresponding point of $p \in F$.
2. Find inlier subset G of F .
 - (a) Sort corresponding pairs (p, q) by $\|T(p) - q\|^2$ in ascending order.
 - (b) Find the first $|G|$ reference points as the inliers from the sorted pairs that minimize E_1 .
3. Compute similarity transformation T that minimizes E_r using correspondence of points in G .
4. Apply T on all points of F .

Plane-fitting registration finds the similarity transformation T that minimizes E_r in Eq.3.3. The algorithm is summarized in Algorithm. 3.1.

The second step and the fourth step of plane-fitting registration is the same as those of FICP. In the first step, for a mesh vertex $p \in F$, its corresponding point $q \in D$ is the closest point of p . On the other hand, for a landmark $q \in L$, its corresponding point p of the reference model is the orthogonal projection of q on the symmetric plane P_F of the reference model. Let us denote the set of points of the reference model and plane p as P , and the set of corresponding points q as Q .

In the third step, E_r can be rewritten as

$$E_r = \sum_{p \in P} w_p^2 \|s\mathbf{R}p + \mathbf{t} - q\|^2 \quad (3.4)$$

where:

$$w_p^2 = \begin{cases} \left(\frac{|F|}{|G|}\right)^\lambda \frac{1}{|G|}, & \text{for } p \in G \\ \frac{1}{|L|}, & \text{for other } p \end{cases}$$

An unweighted version of E_r can be solved using Horn *et al.*'s algorithm [Hor87, HHN88]. Intuitively, a point with integer weight can be considered as corresponding to multiple points at the same position. If the weights are not integer, they can be converted approximately to integer by dividing them by their greatest common divisor. Based on this intuition, we know that the weighted version is similar to the unweighted version and thus it is solvable. We use the implementation from [Pap06] to solve this problem.

Plane-fitting registration algorithm can converge to local minimum because registration error E_r decreases in each step of the iteration. In the first step, finding closest points for mesh vertices would reduce E_1 , because the new closest points for vertices in F are closer than the closest points in previous iteration. Finding new corresponding points for planar landmarks also reduces registration error, because the orthogonal projection p on the symmetric plane of reference model is closer to q than the previous corresponding point on the same plane. In the second step, E_r does not increase, because we can keep the original inlier subset to maintain its value. Finally, in the third and fourth steps, the optimal transformation T^* that minimizes E_r (in the form of Eq.3.4) is applied to reference model. Since we can keep the original transformation T such that $T(p) = p$ to keep E_r unchanged and the optimal transformation T^* is usually better than T , E_r usually decreases. Therefore, same as ICP and FICP, plane-fitting registration algorithm converges to local minimum.

3.2 Experiments and Discussions

Experiments were conducted to evaluate plane-fitting registration algorithm on skull models. In the experiments, 32 full normal skull models were used. One of them was used as

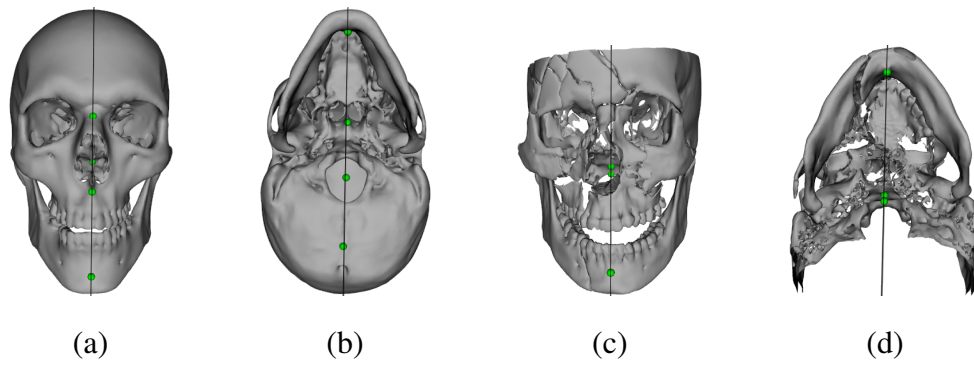


Figure 3.1: Skull Models. (a, b) normal skull model. (c, d) fractured skull model. Green landmarks are planar landmarks that should lie on the symmetric plane (grey lines).

the reference (Fig. 3.1a). In practice, target skulls are usually patients' skulls with deformities. For this reason, 5 skulls were manually cut in a manner similar to real fractures in patients to synthesize five fractured skulls (Fig.3.3(2)). Moreover, 5 skull models of real patients from a local hospital were also used for testing. Fig.3.1c shows an example of a patient's skull. As can be seen, in addition to deformities caused by fracture, real patients' skulls were also incomplete because in practice images are acquired only for the parts of the skulls under treatment.

The resolution of the CT images to generate mesh models ranged from 0.31 to 3 mm/pixel. The CT images were segmented and 3D mesh models were reconstructed from them.

Plane-fitting registration algorithm was applied to register the reference model to all the test target models. For comparison, two popular similarity registration algorithms, ICP [BM92] and FICP [PLT07], were also tested. For fair assessment, the same initialization is performed before executing the registration algorithms.

To quantitatively assess the algorithms, three errors were measured. Surface error E_S measured the root mean-square distance between the corresponding surfaces of two models, and plane-fitting error E_P measured the root mean-square distance from target models' planar landmarks to the reference model's symmetric plane. To examine the convergence of the algorithms, registration errors of one severely fractured skull (Fig.3.3(3)) were mea-

Table 3.1: Comparison of registration methods. E_S denotes surface error (mm), and E_P denotes plane-fitting error (mm). Plane-fitting registration algorithm attained the overall best performance with the lowest plane-fitting error and satisfactory surface error E_S .

Skull Model	ICP		FICP		Plane-fitting	
	E_S	E_P	E_S	E_P	E_S	E_P
Normal	3.63	3.15	3.90	2.93	3.70	0.97
Synthetic	3.83	3.82	4.10	3.27	3.92	1.10
Patient	6.25	9.05	15.38	2.07	14.21	0.86

sured for the intermediate results after each iteration according to the algorithms' objective functions. For ICP, FICP and plane-fitting registration algorithm, the registration errors are mean-square error, fractional mean-square error, and the error E_r shown in Eq.3.3, respectively. Execution time was measured on a PC with a 3.4GHz CPU.

Fig.3.3 shows skull registration results. ICP algorithm was able to find reasonable results for normal skulls (Fig.3.3(1)). However, ICP registration results were greatly affected by outliers caused by incompleteness and fractures of fractured models. Synthetic fractured skulls and real fractured skulls were not properly aligned by ICP algorithm (Fig.3.3(2-5)). For the case in Fig.3.3(3), ICP shrunk the reference model to a small region, and failed to find reasonable alignment between the reference and the patient's model. Due to inaccurate alignment, the symmetric plane of the reference model were not accurately aligned with the planar landmarks of patients' models. In all the three categories of skull models, ICP had the lowest surface error E_S because it minimized the distance for the full set of points even a portion of them are outliers in synthetic and patient models. However, ICP did not take in account symmetric plane-fitting, resulting in large plane-fitting error E_P (Tab.3.1).

FICP was robust to outliers and aligned the reference model relatively well to synthetic and patients' models (Fig.3.3). FICP had larger surface error E_S (Tab.3.1) than ICP algorithm, because it identified a portion of outliers and did not take them into ac-

count. Therefore, errors of the outliers may be arbitrarily large and result in large E_S , even though the overall shape and the inliers are properly registered. This contradiction shows that surface error E_S is not a stable assessment of registration quality. Alignment between the reference model's symmetric plane and the patient models' planar landmarks were not accurate and has large plane-fitting error E_P (Tab.3.1), because FICP did not consider plane-fitting in the registration process.

Plane-fitting registration algorithm inherited its robustness from FICP. In addition to robustly registering the reference models to the target model, it also matched the symmetric plane of the reference model to the patients' planar landmarks accurately (Fig.3.3). It was more robust to outliers than FICP due to the fitting of symmetric plane. The outliers that violated the fitting of plane were also identified and excluded from the computation of similarity transformation. Therefore, the symmetric plane of the reference model was aligned accurately to the patients' planar landmarks, and the inlier surface points were robustly registered, resulting in the lowest plane-fitting error and similar surface error compared to FICP (Tab.3.1).

Fig. 3.2 shows the convergence curves of the three algorithms on a patient's skull (Fig. 3.3(3)). The convergence curves validate that ICP (grey) and FICP (red) converge quickly to local minimum. FICP had smaller registration error after convergence than ICP does, because FICP identified point pairs with large error as outliers and excluded them from registration error computation. The convergence curve of plane-fitting registration algorithm (blue) shows that plane-fitting registration algorithm also converged quickly to local minimum after a few iterations. Plane-fitting registration algorithm had larger registration error than FICP method, because its registration error contained an additional plane-fitting error term besides the fractional mean-square error of FICP.

In all the experiments, the convergence condition is to terminate when the reduction of registration error in a iteration is smaller than 1%. For the model in Fig. 3.3(3), ICP converges within 52 iterations and 0.48 second, FICP converges within 27 iterations and 0.60 second, and plane-fitting registration algorithm converges within 45 iterations and 1.01 second. The algorithm is about 0.5 second slower than the other two algorithms,

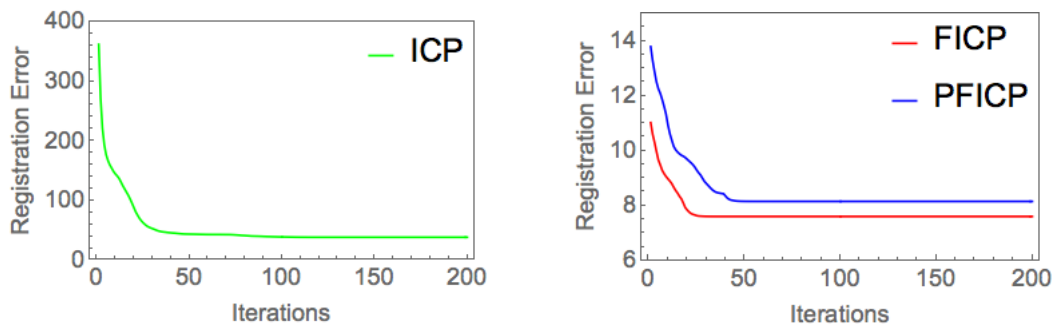


Figure 3.2: Convergence curves. Same as ICP (green) and FICP (red), plane-fitting registration algorithms (blue) converges to a stable value quickly.

which is worthy considering the significant improvement in robustness and registration quality.

3.3 Summary

Existing similarity registration methods such as ICP and FICP are not able to register skull models properly. Plane-fitting registration algorithm is more robust than existing registration algorithms. It achieves its robustness by ensuring that the symmetric plane of the reference model is registered to the planar landmarks of the target model. Quantitative and qualitative experimental results on real patients' skull models show that plane-fitting registration algorithm is efficient and can robustly align the overall structure of the models while matching the symmetric plane of reference model and planar landmarks of target model accurately.

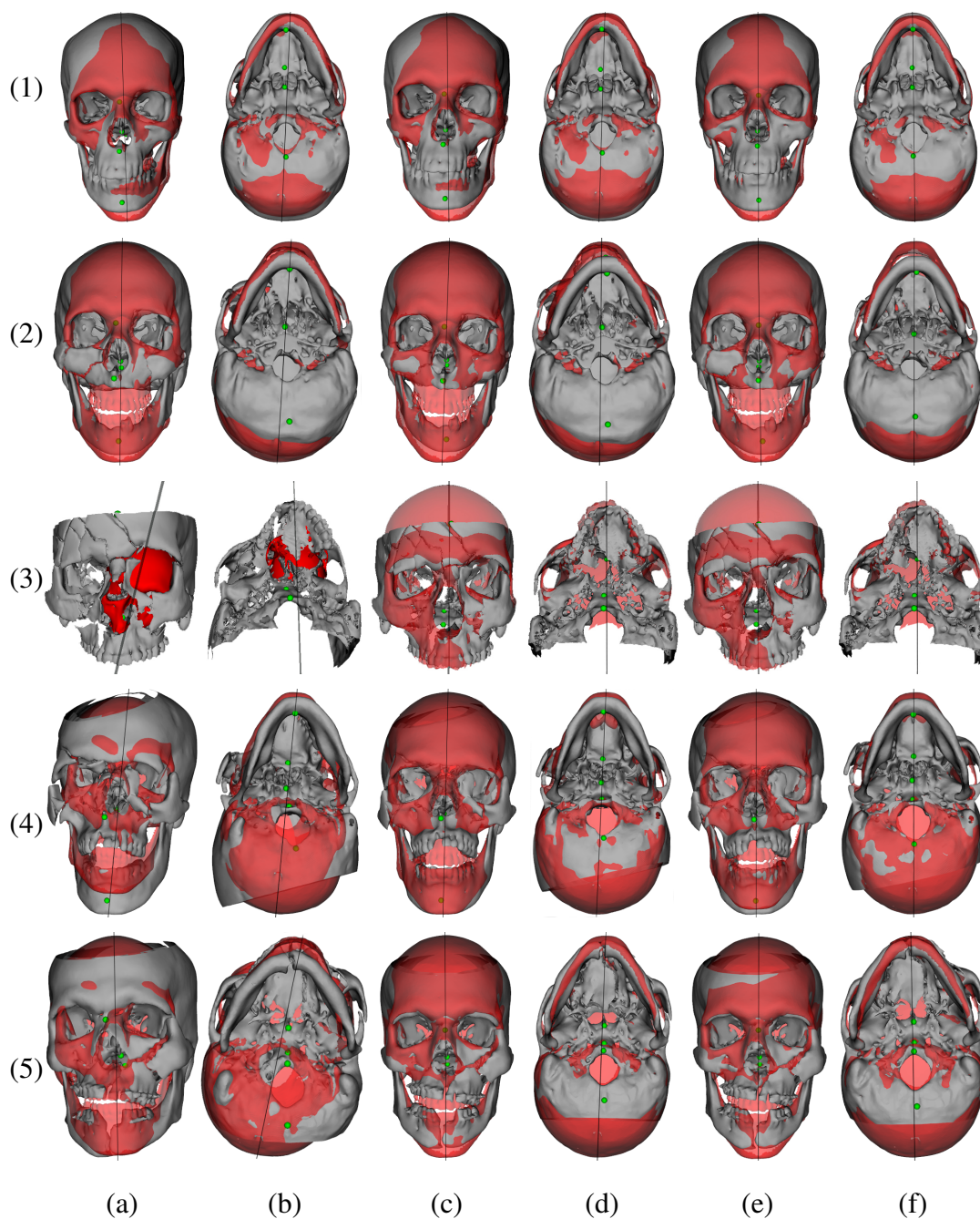


Figure 3.3: Skull registration results. (1) normal skull. (2) synthetic fractured skull. (3-5) patients' fractured skulls. (a, b) ICP. (c, d) FICP. (e, f) plane-fitting registration algorithm. Plane-fitting registration algorithm attained the best overall performance compared to ICP and FICP. It aligned the reference skull models' symmetric planes (grey lines) accurately to the target skull models' planar landmarks (green dots). Surfaces of the reference models are colored red and the target models are colored grey.

Chapter 4

Salient Surface Detection

To ensure the surface continuity, the salient surfaces of the reconstructed skull should flush with salient surfaces of normal parts of the deformed skull. This chapter presents two algorithms for automatic salient surface detection and discusses their accuracy.

4.1 Salient Surface Detection Algorithm

Salient surfaces are important surfaces that are required by surface continuity reconstruction. They include outer surfaces of a skull model that can be easily identified automatically, and surfaces around eye sockets and other openings that are difficult to detect (Fig. 1.3).

The outer surface detecting algorithm is based on the property of outer surface that a ray going from the centroid of the model to a point on the outer surface does not intersect with any other surfaces outside the outer surface. This algorithm cannot detect salient surfaces around eye sockets and other openings, as most of vertices around them do not satisfy the outer surface property.

To detect the whole salient surfaces including outer surfaces and surfaces around eye sockets and other openings, two algorithms are proposed and their accuracy are verified

Algorithm 4.1: Salient Surface Detection 1

1. Apply plane-fitting registration to register the reference model whose salient surfaces are manually marked to the target model.
2. Search target model for salient surface vertices. For each vertex v_i on salient surfaces of the reference model, find its closest vertex v'_i on the target model. Mark v'_i as a salient surface vertex if surface normals at v_i and v'_i are similar.
3. Extend salient surface vertices. For each salient surface vertex on the target model, search vertices with similar surface normals nearby, and mark them as salient surface vertices.
4. Close up the salient surfaces.
5. Find the maximally connected component for each bone of the model.

in Sec. 4.2. The first algorithm (Algorithm 4.1) transfers the outer surfaces and surfaces around eye sockets and other openings from the reference model to the target model, while the second algorithm (Algorithm 4.2) detects outer surfaces for the target model and transfers surfaces around eye sockets and other openings from the reference model to the target model.

Benchmark test in Chap. 3 shows that plane-fitting registration algorithm is more robust than ICP and FICP. So, plane-fitting registration is used for rigid registration in the proposed algorithms.

4.2 Experiments and Discussions

Experiment is conducted to evaluate the accuracy of Algorithm 4.1 and Algorithm 4.2.

Algorithm 4.2: Salient Surface Detection 2

1. Mark outer surfaces of the target model using the outer surface detecting algorithm.
2. Apply plane-fitting registration to register the reference model whose surfaces around eye socket and other openings are manually marked to the target model.
3. Search target model for eye socket vertices. For each vertex v_i on surfaces around eye sockets and other openings of the reference model, find its closest vertex v'_i on the target model. Mark v'_i as a salient surface vertex if surface normals at v_i and v'_i are similar.
4. Extend salient surface vertices. For each salient surface vertex on the target model, search vertices with similar surface normals nearby and mark them as salient surface vertices.
5. Close up the salient surfaces (Fig. 4.1).
6. Find the maximally connected component for each bone of the model

In the experiment, 5 normal, 5 fractured and 1 congenitally deformed skull models are used. One of the normal models is used as the reference model. The salient surfaces of the reference model are manually marked. It is impossible to measure the accuracy exactly without knowing the ground truth, since salient surfaces are not uniquely defined. So, instead of quantitative analysis, qualitative analysis is performed to evaluate the accuracy of two algorithms.

Fig. 4.2 illustrates the registration results. As can be seen in Fig. 4.2, salient surfaces detected by the outer surface detecting algorithm contained only the outer surfaces. For those around eye sockets, it could not detect them, as vertices on surfaces around eye sockets do not satisfy the outer surface property.

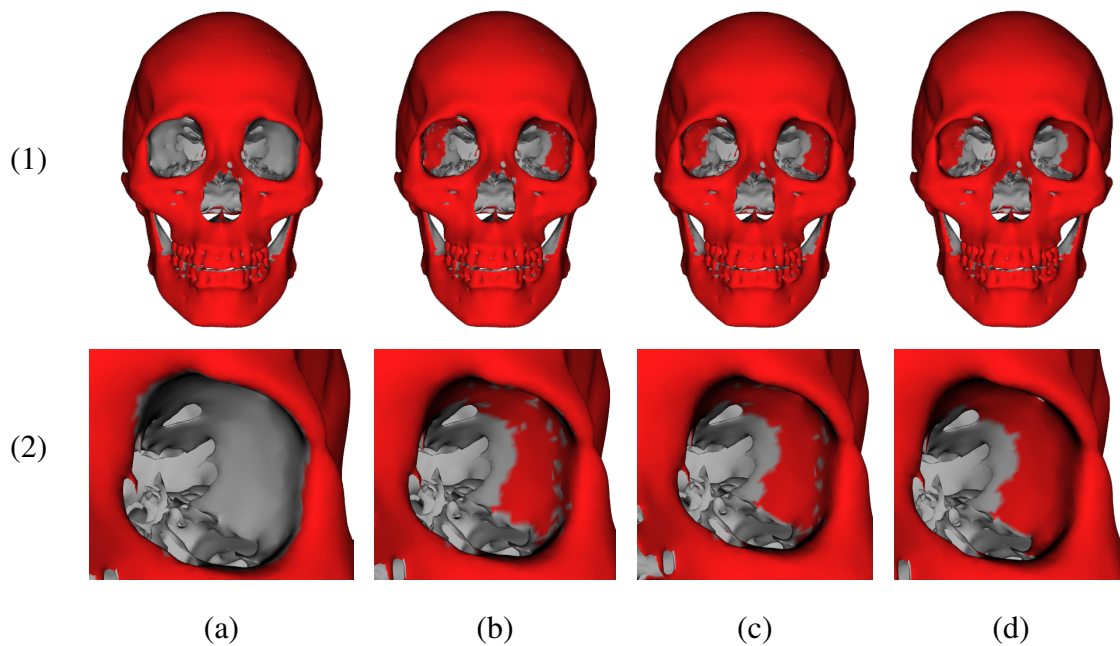


Figure 4.1: Algorithm 4.2 for automatic salient surface detection. (1) overall view. (2) left eye view. (a) outer surface. (b) vertices around eye sockets are found. (c) vertices on salient surfaces are extended. (d) salient surfaces are closed up.

Fig. 4.2 also shows that Algorithm 4.1 does not work well for the testing cases. For the normal skull model, Algorithm 4.1 can detect its upper surfaces well but failed to detect surfaces on its lower jaw. For the deformed model and the fractured model, most of the salient surfaces are not detected by the algorithm. This may be because of two reasons. Firstly, some parts of the reference model do not fit the target model well, especially in the deformed case. Secondly, in step 2, a vertex on salient surfaces of the reference model may not have similar normal with its closest point and its closest point is discarded.

Also, it is notable to see from Fig. 4.2 that the overall salient surfaces of the testing models are well detected by Algorithm 4.2. For the normal model, the detecting result is almost perfect. For the deformed model, surfaces around its right eye sockets are not detected well. This may be because the closest point in step 3 may not have similar normal with the salient surface vertex and is discarded. For the fractured model, salient surfaces around its left eye sockets are identified successfully, while surfaces around its right eye sockets are failed to detect. This is because when the algorithm looks for the closest point

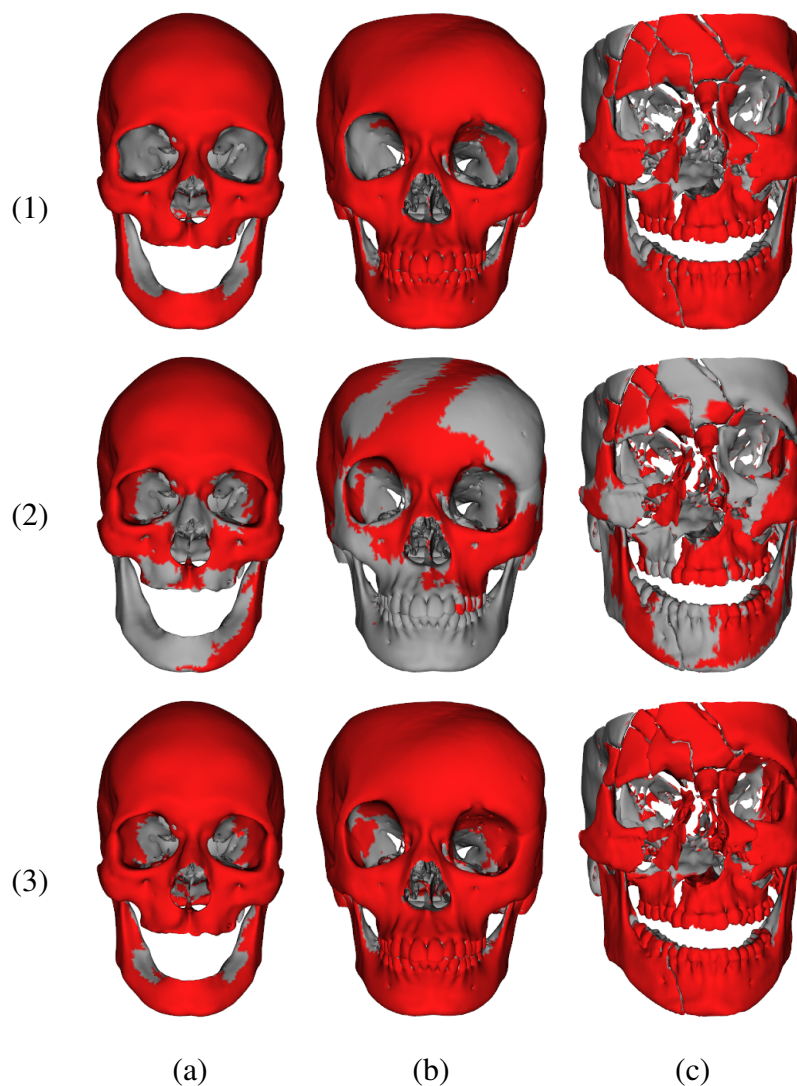


Figure 4.2: Selective salient surface extraction results. (1) Salient surfaces detected by outer surface detecting algorithms. (2) Salient surfaces detected by Algorithm 4.1. (3) Salient surfaces detected by Algorithm 4.2. (a) Normal skull model. (b) Deformed skull model. (c) Fractured skull model. The outer surface detecting algorithm is not able to detect surfaces around eye sockets. Algorithm 4.1 does not work well. Algorithm 4.2 detects both the outer surfaces and surfaces around eye sockets well.

on the target model for the salient surface vertex on the reference model, the point found by the algorithm is usually on the fractured fragment which is close to the eye sockets. Instead of looking for only one closest point, searching for vertices within a small region

and picking the one with the most similar normal as salient surface vertex may solve this problem. Anyway, Algorithm 4.2 can be considered as a promising algorithm for salient surface detection according to the experiment result.

According to the observation, two techniques can be adopted to improve the proposed algorithms. Firstly, the reference model can be deformed using non-rigid registration to fit the target model better, which should increase the detecting accuracy. Secondly, for each vertex on the salient surfaces of the reference model, instead of finding only one closest point on the target model, search vertices of the target model within a range and mark the one with the most similar normal as the salient surface vertex. The improvement will be studied in future work.

4.3 Summary

Salient surfaces are important features used for surface continuity reconstruction. The outer surface detecting algorithm can only detect outer surfaces but is not able to detect salient surfaces around eye sockets and other openings. This chapter proposed two algorithms for automatic salient surfaces detection. According to the experiment result, Algorithm 4.1 does not perform well and Algorithm 4.2 is more accurate in detecting salient surfaces of the tested skull models. So, Algorithm 4.2 can be considered a promising algorithm for salient surface detection for now. Improvement on the proposed algorithms will be studied in continuing work to achieve higher accuracy.

Chapter 5

Continuing Research

There are many problems to be solved in the continuing research for reconstruction of deformed skulls, such as non-rigid registration, improved algorithms for salient surface detection, and balancing of Eq. 3.3.

5.1 Non-rigid registration

Non-rigid registration rotates, translates, scales and deforms a reference model to match the shape of target model. The information provided by the reference model can be better applied to the target model after non-rigid registration. For example, [ZCL13] applies non-rigid registration on a reference model to match the shape of the target model in order to utilize the shape information better to build correspondence between them. Moreover, non-rigid registration may be able to replace rigid registration in the algorithms proposed in Chapter 4 to achieve more accurate result. Non-rigid registration will be studied in the future research.

5.2 Salient Surfaces Detection

In Chapter 4, the accuracy of two proposed algorithms could be improved. Firstly, it is promising to deform the reference model to better match the shape of the target model by replacing rigid registration with non-rigid registration. Secondly, for each vertex on the salient surfaces of reference model, instead of finding only one closest point on the target model, search vertices within a small range and pick one with the most similar normal as salient surface vertex for the target model. These two improvements could potentially increase the accuracy of the proposed algorithms.

5.3 Weighting Parameter

An error function is discussed in Chapter 3:

$$E_r = \alpha E_1 + E_2$$

Determining the weighting parameter α is challenging. This balancing problem will be studied in the continuing work.

5.4 Reconstruction of Deformed Skulls

To develop an accurate and robust reconstruction method for deformed skulls, at least the following components are needed.

- **Plane-fitting rigid registration.** The benchmark test in Chapter 3 shows that plane-fitting rigid registration is more robust than ICP and FICP on deformed skulls. So, it is promising for deformed skull alignment.
- **Non-rigid registration.** Non-rigid registration can be used for building correspondence between skulls, transferring salient surfaces, and estimating normal shapes for fractured or missing parts, all of which are useful for deformed skull reconstruction.

- **Statistical shape model.** A statistical shape model provides information about variations of normal human skulls, which is useful for deformed skull reconstruction.
- **Salient surfaces.** The salient surfaces of the reconstructed skull should be flushed with salient surfaces of normal parts of the deformed skull. It is significant to extract salient surfaces automatically.

Chapter 6

Conclusion

Skull reconstruction is significant for surgery in improving patients' quality of life, forensics in individual identification, and archeology in analyzing the morphology of ancient skulls. However, skull reconstruction is difficult for experts and computation due to the skull complexity and the unknown normal shape corresponding to the fractured or missing part.

Existing approaches for skull reconstruction include symmetry-based reconstruction, geometric reconstruction, and statistical reconstruction. Symmetry-based reconstruction is a simple and useful approach that is widely used in computer-aided systems and has been successfully applied to many real cases. But it cannot be applied directly to a deformed skull with bilateral defects. Geometric reconstruction is applicable to skulls with bilateral deformities, and it overcomes the limitation of symmetry-based reconstruction. However, it uses a single reference model, which is not enough for reconstructing skulls because detailed shapes of human skulls differ significantly with different identifies, genders, ages and races. Statistical reconstruction builds statistical model from a set of training models, which enables it to handle significant variation of human skulls. But it focuses on global structures rather than details of local features, which may lead to mismatches between normal parts of the input skull and the reconstructed skull, causing the loss of local shape information.

Many existing work about skull reconstruction involves rigid registration. Rigid registration must be robust to deformed skull models, as its accuracy affects the accuracy of the reconstruction result. Also, after reconstruction, the salient surface of the filled-in part should be flushed with salient surfaces of the deformed skull to ensure **surface continuity**. Inspired by these important facts, I have done some preliminary work to start this research.

Firstly, benchmark test is performed on ICP, FICP and plane-fitting registration to see which method is the most robust for skull registration. Experiment shows existing similarity registration methods such as ICP and FICP are not able to register skull models properly and plane-fitting registration is efficient and can robustly align the overall structure of the models while matching the symmetric plane of reference model and planar landmarks of target model accurately.

Secondly, the accuracy of two algorithms for salient surfaces detection are verified. The first algorithm transfers salient surfaces from the reference model to the target model. The second one extracts outer surfaces of the target model and transfers salient surfaces around eye sockets and other openings from the reference model to the target model. Experiment shows that the first algorithm can only detect a small portion of salient surfaces, while the second one can detect almost all the salient surfaces. The second one is thus considered as a promising algorithm for salient surface detection. In the continuing work, promising improvements such as deforming the reference model to match the shape of the deformed model better and finding the salient surface vertex within a region will be studied to enhance the robustness of the proposed algorithms.

All these work can contribute to the future research on reconstruction of deformed skulls.

Bibliography

- [BM92] P.J. Besl and N.D. McKay. Method for registration of 3-d shapes. In *Robotics-DL tentative*, pages 586–606. International Society for Optics and Photonics, 1992.
- [BS11] S. Benazzi and S. Senck. Comparing 3-dimensional virtual methods for reconstruction in craniomaxillofacial surgery. *Journal of Oral and Maxillofacial Surgery*, 69(4):1184–1194, 2011.
- [BSMG09] S. Benazzi, E. Stansfield, C. Milani, and G. Gruppioni. Geometric morphometric methods for three-dimensional virtual reconstruction of a fragmented cranium: The case of Angelo Poliziano. *International Journal of Legal Medicine*, 123(4):333–344, 2009.
- [Che13] Y. Cheng. *Computer-aided craniomaxillofacial surgery planning for fractured skulls*. PhD thesis, National University of Singapore, 2013.
- [CSP⁺07] J. Chapuis, A. Schramm, I. Pappas, W. Hallermann, K. Schwenzer-Zimmerer, F. Langlotz, and M. Caversaccio. A new system for computer-aided preoperative planning and intraoperative navigation during corrective jaw surgery. *Information Technology in Biomedicine, IEEE Transactions on*, 11(3):274–287, 2007.
- [CTCG95] T.F. Cootes, C.J. Taylor, D.H. Cooper, and J. Graham. Active shape models—their training and application. *Computer Vision and Image Understanding*, 61(1):38–59, 1995.

- [CTS⁺10] L.H.C. Cevidanes, S. Tucker, M. Styner, H. Kim, J. Chapuis, M. Reyes, W. Proffit, T. Turvey, and M. Jaskolka. Three-dimensional surgical simulation. *American Journal of Orthodontics and Dentofacial Orthopedics*, 138(3):361–371, 2010.
- [dMCP⁺06] E. de Momi, J. Chapuis, I. Pappas, G. Ferrigno, W. Hallermann, A. Schramm, and M. Caversaccio. Automatic extraction of the mid-facial plane for cranio-maxillofacial surgery planning. *International Journal of Oral and Maxillofacial Surgery*, 35(7):636–642, 2006.
- [FdCP⁺08] M. Fantini, F. de Crescenzo, F. Persiani, S. Benazzi, and G. Gruppioni. 3D restitution, restoration and prototyping of a medieval damaged skull. *Rapid Prototyping Journal*, 14(5):318–324, 2008.
- [GMBW04] P. Gunz, P. Mitteroecker, F.L. Bookstein, and G.W. Weber. Computer aided reconstruction of human crania. *BAR International Series*, 1227:92–95, 2004.
- [Goo91] C. Goodall. Procrustes methods in the statistical analysis of shape. *Journal of the Royal Statistical Society. Series B (Methodological)*, pages 285–339, 1991.
- [Gow75] J.C. Gower. Generalized procrustes analysis. *Psychometrika*, 40(1):33–51, 1975.
- [GWL99] H.K. Gumprecht, D.C. Widenka, and C.B. Lumenta. Brainlab vectorvision neuronavigation system: technology and clinical experiences in 131 cases. *Neurosurgery*, 44(1):97–104, 1999.
- [Hem10] Facts about Hemifacial Microsomia, 2010. <http://www.littlebabyface.org/pdfs/hemifacialMicrosomia.pdf>.
- [HHN88] B.K.P. Horn, H.M. Hilden, and S. Negahdaripour. Closed-form solution of absolute orientation using orthonormal matrices. *JOSA A*, 5(7):1127–1135, 1988.

- [Hor87] B.K.P. Horn. Closed-form solution of absolute orientation using unit quaternions. *JOSA A*, 4(4):629–642, 1987.
- [LAV09] M. Lüthi, T. Albrecht, and T. Vetter. Building shape models from lousy data. In *Medical Image Computing and Computer-Assisted Intervention–MICCAI 2009*, pages 1–8. Springer, 2009.
- [LCL⁺03] M.Y. Lee, C.C. Chang, C.C. Lin, L.J. Lo, and Y.R. Chen. T medical rapid prototyping in custom implant design for craniofacial reconstruction. In *Systems, Man and Cybernetics, 2003. IEEE International Conference on*, volume 3, pages 2903–2908. IEEE, 2003.
- [LP98] J.D. Langdon and M.F. Patel. *Operative maxillofacial surgery*. Chapman & Hall Medical, 1998.
- [LYW⁺11] X. Li, Z. Yin, L. Wei, S. Wan, W. Yu, and M. Li. Symmetry and template guided completion of damaged skulls. *Computers & Graphics*, 35(4):885–893, 2011.
- [Pap06] S. Paperini. `vtkweightedlandmarktransform`, 2006. [Online; accessed 28-October-2014].
- [PLT07] J.M. Phillips, R. Liu, and C. Tomasi. Outlier robust icp for minimizing fractional rmsd. In *3-D Digital Imaging and Modeling, 2007. 3DIM'07. Sixth International Conference on*, pages 427–434. IEEE, 2007.
- [Row98] S. Roweis. Em algorithms for pca and spca. *Advances in Neural Information Processing Systems*, pages 626–632, 1998.
- [TB99] M.E. Tipping and C.M. Bishop. Probabilistic principal component analysis. *Journal of the Royal Statistical Society: Series B (Statistical Methodology)*, 61(3):611–622, 1999.
- [Thi98] J.P. Thirion. Image matching as a diffusion process: an analogy with maxwell’s demons. *Medical Image Analysis*, 2(3):243–260, 1998.

- [WYLL11] L. Wei, W. Yu, M.Q. Li, and X. Li. Skull assembly and completion using template-based surface matching. In *3D Imaging, Modeling, Processing, Visualization and Transmission (3DIMPVT), 2011 International Conference on*, pages 413–420. IEEE, 2011.
- [YWML11] Z. Yin, L. Wei, M. Manhein, and X. Li. An automatic assembly and completion framework for fragmented skulls. In *Computer Vision (ICCV), 2011 IEEE International Conference on*, pages 2532–2539. IEEE, 2011.
- [ZCL13] K. Zhang, Y. Cheng, and W.K. Leow. Dense correspondence of skull models by automatic detection of anatomical landmarks. In *Computer Analysis of Images and Patterns*, pages 229–236. Springer, 2013.
- [Zha14] K. Zhang. Dense correspondence and statistical shape reconstruction of fractured and incomplete skulls. Master’s thesis, National University of Singapore, 2014.
- [ZLES05] S. Zachow, H. Lamecker, B. Elsholtz, and M. Stiller. Reconstruction of mandibular dysplasia using a statistical 3D shape model. In *International Congress Series*, volume 1281, pages 1238–1243. Elsevier, 2005.